

Article

Effect of Sucrose Concentration on *Streptococcus mutans* Adhesion to Dental Material Surfaces

Anamarija Zore ^{1,†}, Franc Rojko ^{1,†}, Nives Matijaković Mlinarič ¹, Jona Veber ¹, Aleksander Učakar ², Roman Štukelj ¹, Andreja Pondelak ³, Andrijana Sever Škapin ^{3,4} and Klemen Bohinc ^{1,*}

¹ Faculty of Health Sciences, University of Ljubljana, Zdravstvena 5, 1000 Ljubljana, Slovenia; anamarija.zore@zf.uni-lj.si (A.Z.); matijakovicn@zf.uni-lj.si (N.M.M.)

² Jozef Stefan Institute, Jamova 39, 1000 Ljubljana, Slovenia

³ Slovenian National Building and Civil Engineering Institute, 1000 Ljubljana, Slovenia

⁴ Faculty of Polymer Technology—FTPO, Ozare 19, 2380 Slovenj Gradec, Slovenia

* Correspondence: klemen.bohinc@zf.uni-lj.si; Tel.: +386-1300-1170

† These authors contributed equally to this work.

Abstract: Enamel demineralization, known as dental caries, is instigated by the bacterium *Streptococcus mutans*, which generates acid during carbohydrate metabolism. Among carbohydrates, sucrose is the most cariogenic and capable of biofilm formation. This study aimed to explore and comprehend *Streptococcus mutans*' adherence to two prevalent dental material surfaces, i.e., a cobalt–chromium (Co-Cr) alloy and a resin-based composite, under the influence of various sucrose concentrations. To understand bacterial adhesion, the surfaces were characterized using profilometry, tensiometry, and surface charge measurements. Bacterial adhesion was evaluated using scanning electron microscopy and crystal violet dye methods. Results revealed that the composite surface exhibited greater roughness compared with the Co-Cr alloy surface. Both surfaces displayed hydrophilic properties and a negative surface charge. Bacterial adhesion experiments indicated lower bacterial adherence to the Co-Cr alloy than to the composite surface before the addition of sucrose. However, the introduction of sucrose resulted in biofilm development on both surfaces, showcasing a similar increase in bacterial adhesion, with the highest levels being observed at a 5% sucrose concentration in the bacterial suspension. In conclusion, the findings suggest sucrose-rich foods could facilitate bacterial adaptation despite less favorable surface characteristics, thereby promoting biofilm formation.

Keywords: bacterial adhesion; *Streptococcus mutans*; dental material surfaces; sucrose concentration



Citation: Zore, A.; Rojko, F.; Mlinarič, N.M.; Veber, J.; Učakar, A.; Štukelj, R.; Pondelak, A.; Sever Škapin, A.; Bohinc, K. Effect of Sucrose

Concentration on *Streptococcus mutans* Adhesion to Dental Material Surfaces. *Coatings* **2024**, *14*, 165. <https://doi.org/10.3390/coatings14020165>

Academic Editor: Jun-Beom Park

Received: 30 November 2023

Revised: 19 January 2024

Accepted: 23 January 2024

Published: 27 January 2024



Copyright: © 2024 by the authors. Licensee MDPI, Basel, Switzerland. This article is an open access article distributed under the terms and conditions of the Creative Commons Attribution (CC BY) license (<https://creativecommons.org/licenses/by/4.0/>).

1. Introduction

Recently, significant improvements in dental materials have been made. In restorative dentistry, advanced methods and techniques are replacing the established treatments [1]. However, negative consequences on human health need to be addressed before the clinical implementation of new restorative materials [2]. Restorative dentistry encounters a notable prevalence of secondary caries, which emerges at the margins of tooth restorations [3,4]. Establishing optimal contact between the restorative material and the tooth surface stands as a pivotal preventive measure against secondary caries development [5]. The likelihood of secondary caries development is influenced by the choice of restorative material [4], as well as the presence of defects and gaps fostering biofilm formation at the interface between the tooth and the restorative material [6]. Managing bacterial adhesion to novel dental restorative materials within the oral cavity can potentially reduce biofilm formation [7].

Among the most prevalent chronic diseases globally, dental caries involves the localized deterioration of dental tissues triggered by acidic by-products resulting from bacterial carbohydrate metabolism [8]. Caries is a multistep disease beginning with the formation of biofilm. Caries development is influenced by oral hygiene, saliva composition, fluoride exposure, and the frequency of sugar intake. The disease progresses slowly and can affect

the enamel, dentin, cementum, root, and even pulp [9]. The leading cause of caries among bacteria is *Streptococcus mutans* (*S. mutans*), which produces short-chain carboxylic acids that dissolve hard dental tissues. In addition, *S. mutans* can ferment sucrose and produce insoluble extracellular polysaccharides that increase their adhesion to dental surfaces and teeth, thereby promoting biofilm formation [10].

The adhesion of bacteria to dental material surfaces crucially depends on the surface characteristics [11,12]. A two-stage kinetic binding model can present the adhesion. In the first phase, van der Waals, electrostatic, hydrophobic, and contact interactions mainly govern the adhesion of bacteria onto the interface. The second phase includes specific and nonspecific interactions between so-called adhesion proteins expressed on bacterial surface structures and binding molecules on dental material surfaces. The surfaces need to be characterized to understand the experimental results. The surface topography of the material can be measured with profilometry or atomic force microscopy (AFM). Surface hydrophobicity can be determined through contact angle measurement using a tensiometer. The surface charge can be measured with an electrokinetic analyzer. Multiple methods, such as scanning electron microscopy (SEM) for direct bacterial counting or colony forming units (CFU) plate count and dye staining for indirect methods, can be used to assess bacterial adhesion extent [13].

Given their ability to colonize various oral surfaces, oral *Streptococci* significantly influence oral health and disease development [14]. During biofilm development at neutral pH, species such as *Actinomyces* spp., *Streptococcus gordonii*, and *Streptococcus mitis* dominate. However, the presence of sucrose favors the growth of *S. mutans*. The lowered pH in the oral cavity and the production of mutacins by *S. mutans* disrupt the microbial balance, favoring the growth of *S. mutans* and making it the dominant species in the biofilm [15]. Bacterial adhesion and biofilm formation are accentuated in the presence of sugars within bacterial suspensions [16]. The result of pronounced bacterial adhesion is the intensive bacterial fermentation of sugars in food, which induces tooth demineralization through acid releases [17]. The sucrose fermentation process causes a reduction in the concentration of inorganic phosphorus, calcium, and fluoride, which are essential for demineralization and remineralization of tooth enamel [18].

Cobalt–chromium (Co–Cr) alloys find extensive application in removable dental prostheses and orthodontic devices like brackets, arch wires, and bands [19,20]. A clinical study conducted on patients wearing Co–Cr removable dentures for five to six years revealed a direct association between the occurrence of root caries and contact with the Co–Cr dentures [21]. Studies on Co–Cr alloys have demonstrated substantial *S. mutans* adherence, particularly on recast Co–Cr alloys [22]. *S. mutans* attachment to Co–Cr alloys can also cause alloy corrosion due to local acidification, affecting the properties and quality of the material [23].

Conversely, resin-based composites are commonly employed in dental restorations for repairing teeth affected by decay, fractures, or structural issues in both anterior and posterior regions, owing to their durable nature and aesthetic properties [24]. *S. mutans* demonstrates successful adherence to various resin-based composites, including microhybrid Filtek Z250, Filtek Supreme XT, Enamel Plus HRI, Filtek™ Silorane, Tetric EvoCeram® Bulk Fill, and Kalore™, as well as amalgam composites [25–27]. In an extended period of 4.5 to 10 years post-tooth restoration, no significant difference in the performance of various composites regarding the occurrence of secondary caries was observed [28–30]. Furthermore, studies have reported occurrences of secondary caries within two years post-tooth restoration, primarily attributed to marginal adaptation deficiencies and potential contamination by saliva during the restoration process [31].

This work aimed to investigate how sucrose concentration in a suspension impacts the extent of bacterial adhesion by *S. mutans* to two common dental material surfaces, i.e., a Co–Cr alloy and a resin-based composite, which has not been explored to date. For this reason, the surface characteristics of both material surfaces were measured. The roughness was determined with profilometry; hydrophobicity, with contact angle measurements; and

the zeta potential, with kinetic analyzer measurements. The bacterial adhesion extent under different sucrose concentrations was determined from SEM micrographs and the crystal violet dye method. We hypothesize that due to differing surface characteristics, *S. mutans* exhibit more extensive adherence to resin-based surfaces and that the addition of sucrose further augments bacterial adhesion to Co-Cr alloy and composite surfaces.

2. Materials and Methods

2.1. Bacteria

In this study, *S. mutans* ATCC 25175 standard strains were used and selected from culture on blood agar plates, which were incubated at 37 °C for 24 h with a CO₂ pack for microaerobic conditions.

2.2. Material Surfaces

In this study, two types of dental restorative materials were used: Co-Cr alloy- I-BOND NF (Interdent d.o.o., Celje, Slovenija) and a resin-based composite, Microhybrid composite Z250 (3M, St. Paul, MN, USA). The samples were prepared by pouring Co-Cr alloy- I-BOND NF into a mold, followed by cooling and excess-edge trimming. Composite Z250 was pressed into a mold and polymerized under UV light. The samples were cleaned of residues, and the excess edges were removed. Co-Cr and composite surfaces were cast in standard thickness (2 mm) and size areas of 10 × 10 mm for bacterial adhesion analysis and 10 × 20 mm for the surface characterization of materials. Both the Co-Cr alloy and the composite were polished. Each sample was ground on fine dental polishing sandpaper (P400 grit; SIA Abrasives, Frauenfeld, Switzerland) to the appropriate dimensions (mentioned above). The smoothing of the surfaces was conducted with composite (Alphafleks HP; Edenta AG, Switzerland; REF 0044HP-100, LOT I04.001, ISO 658 1 04 243 513 055)/metal (Exa Technique; Edenta AG, Au, Switzerland; REF 0664HP-100, LOT I11.017, ISO 658 1 04 273 534 100) polishing rubber. Afterward, the samples were polished with polishing paste for composite (Diamond Polishing Paste; Interdent, Celje, Slovenia; REF 461, LOT 2023060213)/Co-Cr alloy (Bego Polishing compounds; Bego Canada, Québec, QC, Canada; REF 0460, LOT 40012840) to a high gloss. Then, the samples were cleaned in an ultrasonic bath. For bacterial adhesion experiments, the samples were sterilized after polishing in an autoclave at 121 °C for 15 min.

2.3. Surface Characterization

Profilometry was used to measure the surface topography. Materials were analyzed with the mechanical profilometer Form Talysurf Series (Taylor-Hobson Ltd., Leicester, UK) in triplicates by vertically measuring the profile of the material's surface with 3 nm resolution in five repetitions. The material roughness and waviness were distinguished by applying a Gaussian filter of 0.8 mm. On the surface of each sample, at least three-line measurements of the length of 5 mm were performed, and the root mean square roughness (R_q) and the arithmetic average roughness (R_a) were determined.

The tensiometer Attension Theta (Biolin Scientific, Gothenburg, Sweden) was used to measure the water contact angles on both surfaces in five replicates.

To obtain information about the surface potential, the streaming potential was measured. An electrokinetic analyzer (SurPASS; Anton Paar GmbH, Graz, Austria) was used. The surface potential measurements were performed in a pH range between 3 and 6 at room temperature in 1 mM phosphate-buffered saline (PBS) solution. Nitrogen gas was continuously purged through the electrolyte solution after the preparation and during the measurement to avoid the dissolution of CO₂ in the solution.

2.4. Monitoring *S. mutans* Growth and Adhesion Extent

The *S. mutans* overnight culture was made in brain–heart infusion (BHI) nutrient broth (Biolife, Italiana Srl, Monza MI, Italy) (4012302) and incubated at 37 °C for 18 h to obtain 10⁹ CFU mL⁻¹ bacterial suspension. The overnight bacterial suspension was diluted 1:300

to a proximal cell concentration of 10^7 CFU mL⁻¹ in a fresh BHI nutrient broth. In this suspension, different concentrations of sucrose (0%, 1.5%, 2.5%, and 5%) were added.

The bacterial adhesion extent was monitored on Co-Cr alloy and composite surfaces. First, specimens (10 × 10 mm) of each material were immersed in artificial saliva [32] for one hour. Then, the specimens were transferred into the diluted (1:300) overnight culture of *S. mutans* in BHI broth with and without sucrose. Specimens were incubated for 10 h, and afterward, the non-adhered cells were washed off three times with 5 mL of 1 M sterile phosphate-buffered saline (PBS buffer). The washed surfaces were used in scanning electron microscopy (SEM) and staining methods for the determination of adhered bacteria. Each experiment was conducted in 8 replicates.

In the SEM method, the adhered bacteria were determined by analyzing SEM micrographs applying the procedure by Nozaki et al. [33] with some modifications. The adhered bacteria were fixed on the Co-Cr alloy and composite with hot air at 60 °C for 10 min. Afterward, a thin gold layer (7 nm) was applied to the surfaces with adhered bacteria to achieve a conductive sample by using the GATAN Model 682 PECS system (Precision Ion Etching and Coating System; GATAN Inc., Pleasanton, CA, USA). The surfaces were analyzed with SEM Jeol JSM-7600F (Jeol, Tokyo, Japan). Afterward, the SEM images were analyzed with ImageJ software (Version 1.50b, 2015; Wayne Rasband, National Institutes of Health, Bethesda, MD, USA). In the obtained SEM micrographs, the bacteria were manually encircled for quantitative analysis.

In the crystal violet staining method with absorbance measurement, samples were stained with 0.04% crystal violet (Merck KGaA, Darmstadt, Germany), incubated at room temperature for 5 min, then washed three times with 5 mL of 1 M sterile PBS buffer, and dried with a hair dryer for 10 min. Stained surfaces without the bacteria were used as the negative control. On the stained surfaces, 400 µL of 96% ethanol was added. A volume of 200 µL of ethanol solution above the stained surfaces was pipetted into a microtiter plate with 96 wells. The optical density of the eluted solution was measured with a spectrophotometer (Tecan, Mannedorf/Zürich, Switzerland) at a wavelength of 620 nm. Measurements were performed for 0%, 1.5%, and 2.5% sucrose concentrations.

The influence of sucrose on the growth curves of *S. mutans* bacterial suspension was studied in BHI broth with different sucrose concentrations (0%, 1.5%, and 2.5%) in triplicates. The overnight bacterial solution was diluted to 10^4 CFU mL⁻¹ and incubated between 0 and 24 h in a microtiter plate (96 wells). Bacterial growth was determined with optical density measurements (with microplate reader Tecan; Mannedorf/Zürich, Switzerland) at 620 nm. Additionally, the number of live bacteria in the incubated suspensions was checked by spotting a series of dilutions (20 µL) on a BHI agar plate and counting the colony-forming units after 24 h of incubation of the agar plate at 37 °C. We used a culture medium without *S. mutans* bacteria as a negative control.

3. Results

3.1. Roughness

The roughness of both considered dental materials was analyzed with the mechanical profilometer. Figure 1a shows the arithmetic average roughness (R_a) for both material dental surfaces. The roughness of the Co-Cr alloy ($R_a = 0.21 \mu\text{m} \pm 0.03 \mu\text{m}$) was lower than the roughness of the composite ($R_a = 0.32 \mu\text{m} \pm 0.06 \mu\text{m}$). Figure 1b shows the root mean square roughness (R_q). The results were similar to R_a , with Co-Cr alloy roughness ($R_q = 0.26 \mu\text{m} \pm 0.03 \mu\text{m}$) being lower than the roughness of the composite ($R_q = 0.41 \mu\text{m} \pm 0.05 \mu\text{m}$).

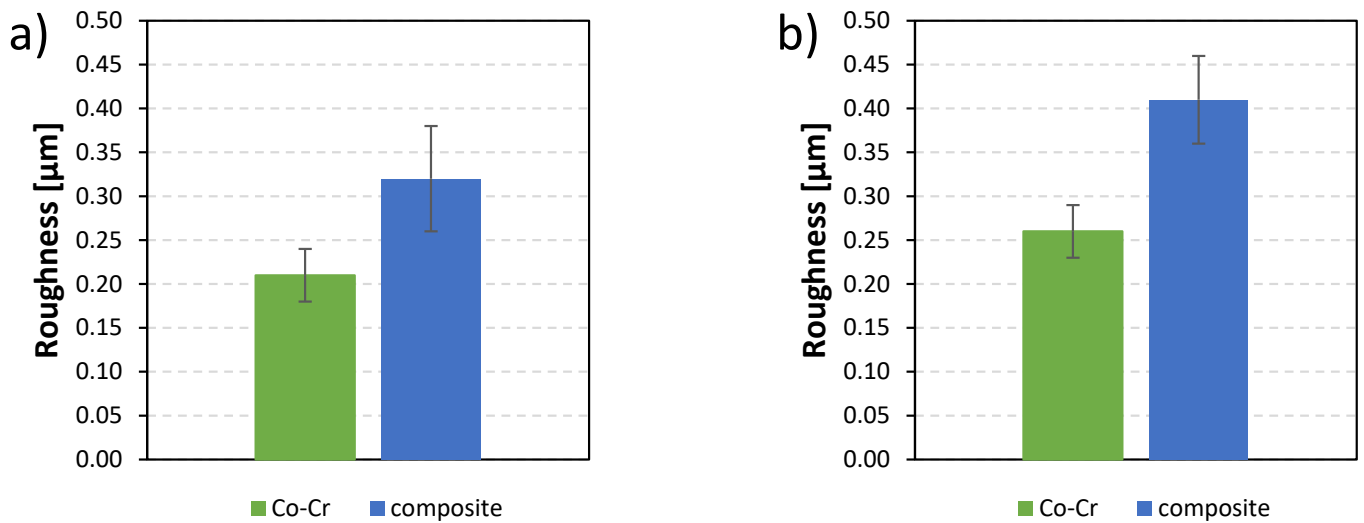


Figure 1. The roughness of two dental material surfaces, Co-Cr alloy and composite: (a) arithmetic average roughness (R_a) and (b) root mean square roughness (R_q).

3.2. Contact Angle

The contact angles of a water droplet on both dental material surfaces were measured with an optical tensiometer. For both surfaces, several measurements were performed, and the average contact angles with their standard deviation were calculated. Figure 2 shows the contact angles of the Co-Cr alloy ($76.63^\circ \pm 0.5^\circ$) and the composite ($74.10^\circ \pm 0.5^\circ$). Both surfaces were hydrophilic.

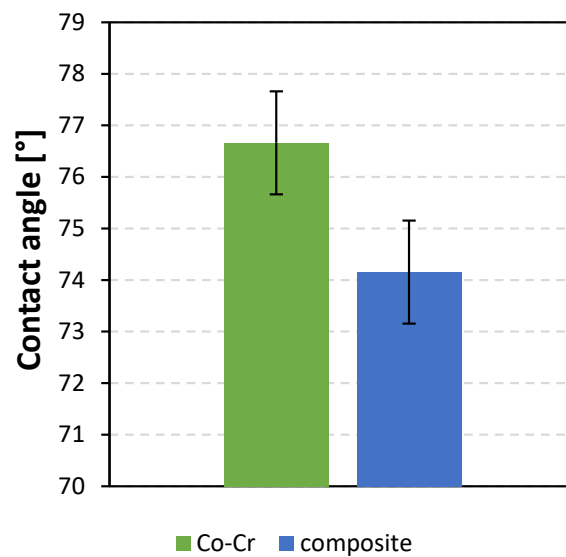


Figure 2. Contact angles of water droplet on dental materials: Co-Cr alloy and composite.

3.3. Zeta Potential

The zeta potential measurements (Figure 3) indicate that at lower pH, surfaces were positively charged, whereas at higher pH, surfaces were negatively charged. The isoelectric point of the Co-Cr alloy was at pH = 3.1, whereas the isoelectric point of the composite's surface was at pH = 4.5.

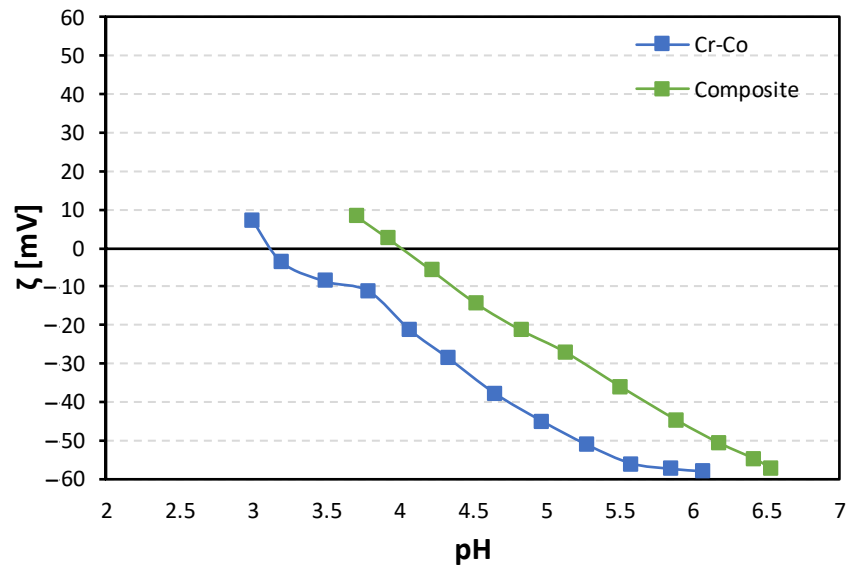


Figure 3. Zeta potential as a function of pH of two dental surfaces: Co-Cr alloy and composite.

3.4. Bacterial Adhesion Extent

Figure 4 shows the bacterial adhesion extent, which is defined as the ratio between the surface area covered by bacteria and the total surface area of the material. Results are shown for both types of surfaces: Co-Cr and composite. The highest percentage of coverage was obtained for the composite with 5% sucrose ($93.94 \pm 0.03\%$), and the lowest percentage, for Co-Cr without sucrose ($5.94 \pm 0.02\%$). The Co-Cr and composite surfaces did not exhibit significant differences in bacterial adhesion extent at the same sucrose concentration.

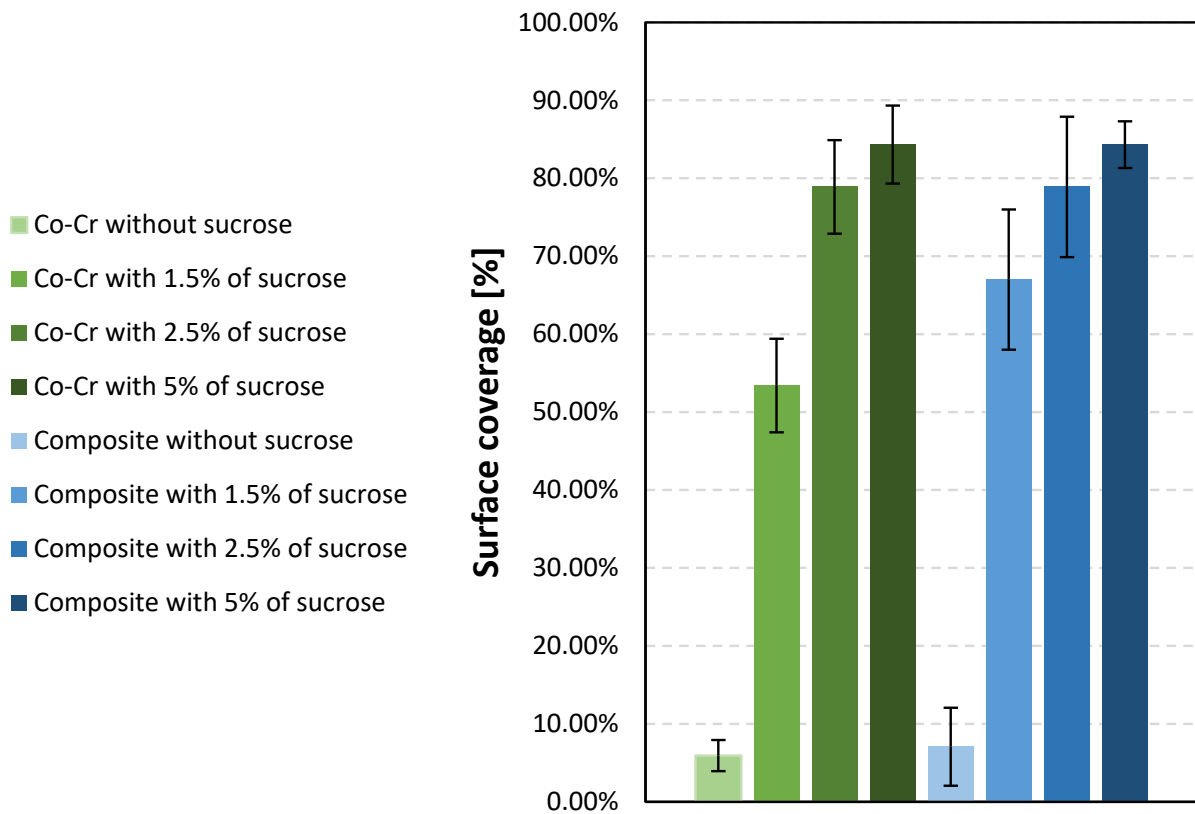


Figure 4. Percentage of surface covered by bacteria for both types of material. Results are shown for three different concentrations of sucrose. Also, results without added sucrose are shown.

Figure 5 shows the absorbance of crystal violet extracted from bacterial cells adhered to the Co-Cr and composite surfaces. The highest absorbance was measured for the bacteria adhered to the composite surfaces with 2.5% sucrose (0.43 ± 0.04), and the lowest, for Co-Cr surfaces without sucrose (0.13 ± 0.06). Lower absorbance was measured on surfaces immersed in a solution without sucrose than on those in solutions with added sucrose. Before the addition of sucrose, the lowest bacterial adhesion extent was measured on Co-Cr surfaces, and the largest, on composite surfaces. However, bacterial adhesion was similar for both surfaces after sucrose addition.

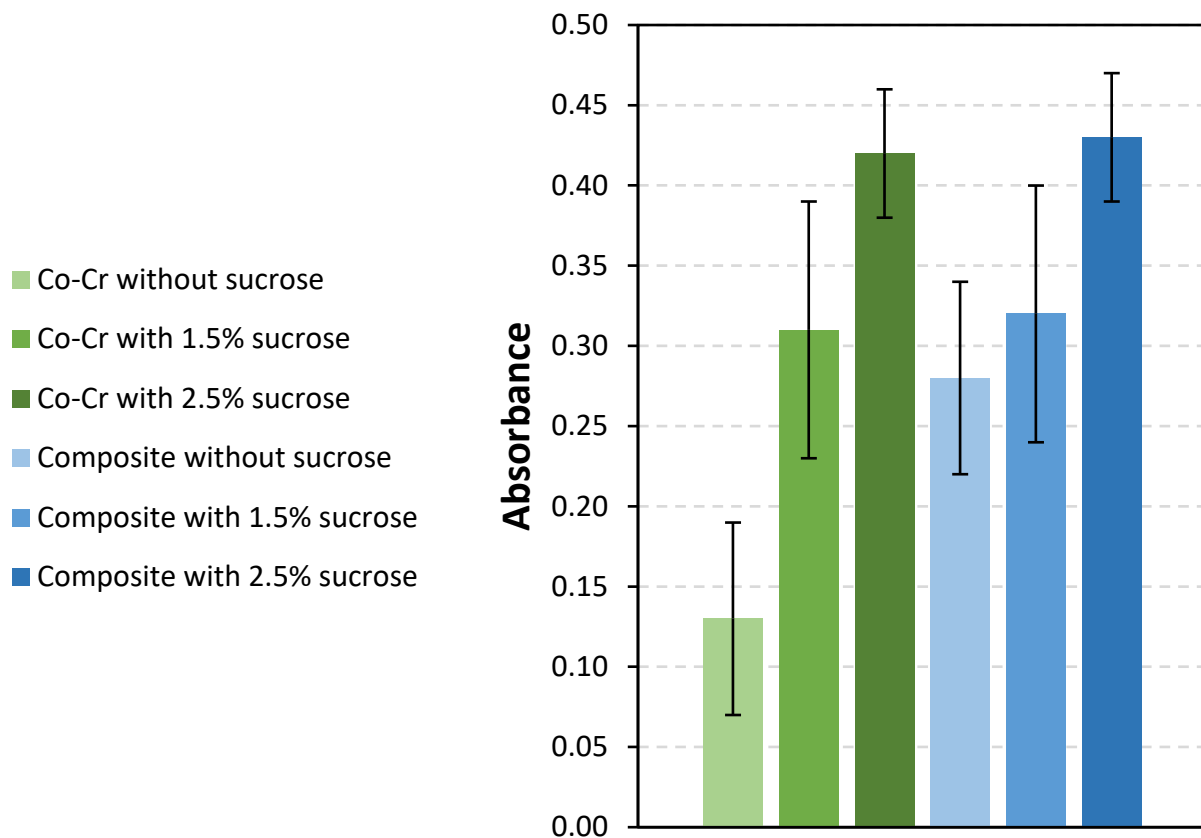


Figure 5. Absorbance at 620 nm for both materials and three sucrose concentrations. Also, results without added sucrose are shown.

SEM was used to image the surfaces of the samples with adhered bacteria and to determine where the bacteria had adhered. Bacterial adhesion to dental surfaces that were incubated for 14 h was evaluated using a series of SEM micrographs (Figures 6 and 7). Figure 6 shows a collage of micrographs of *S. mutans* adhered to the Co-Cr surface at the following sucrose concentrations: 0% (1), 1.5% (2), 2.5% (3), and 5% (4). Figure 7 shows a collage of micrographs of *S. mutans* bacteria on the surface of the composite at the following sucrose concentrations: 0% (a), 1.5% sucrose (b), 2.5% sucrose (c), and 5% sucrose (d). A smaller part of the surface was covered with bacteria at lower sucrose concentrations. On the contrary, more adhered bacteria were observed at higher sucrose concentrations.

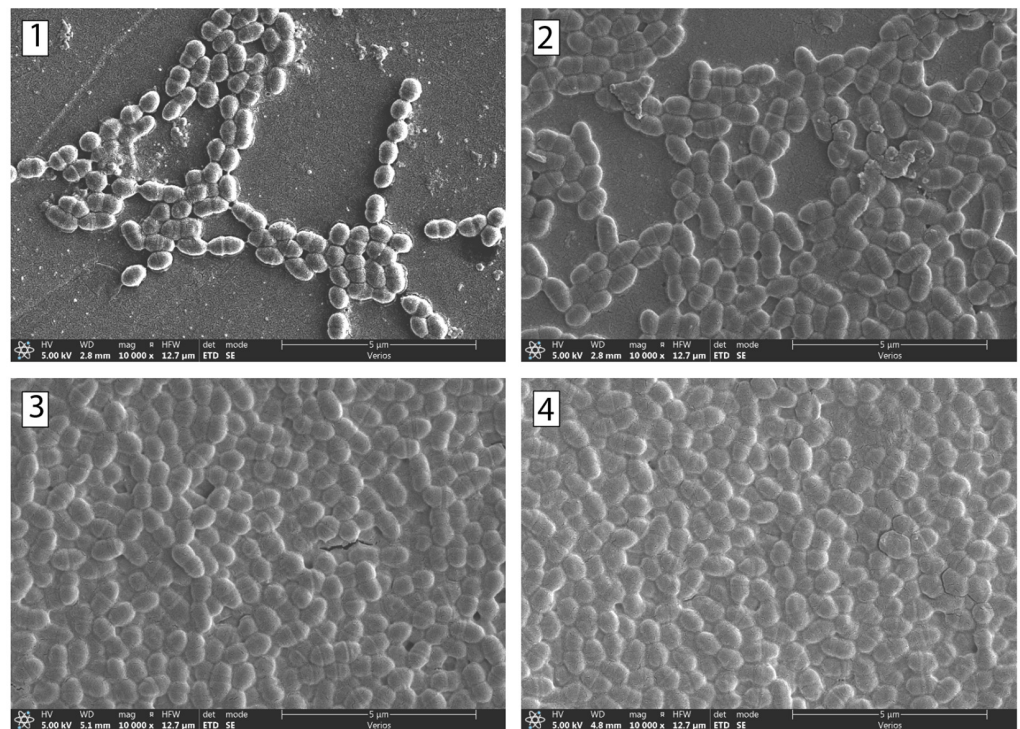


Figure 6. SEM micrographs of the bacteria *S. mutans* after 14 h of incubation time. The micrographs are of Co-Cr surfaces with the following sucrose concentrations: (1) 0%, (2) 1.5%, (3) 2.5%, and (4) 5%.

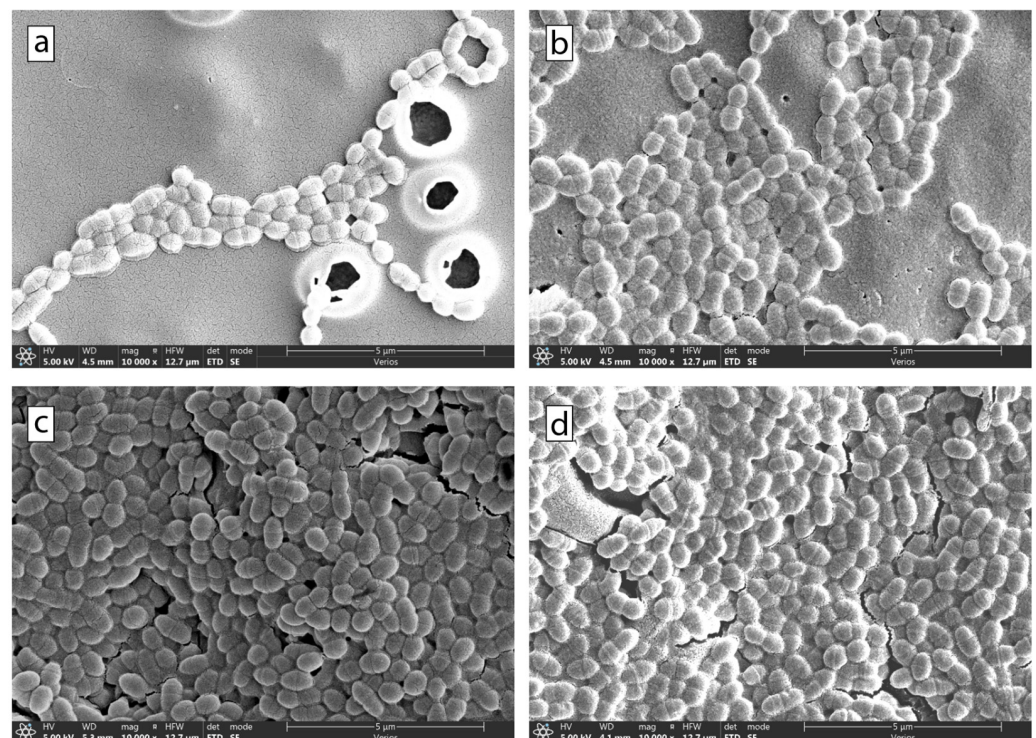
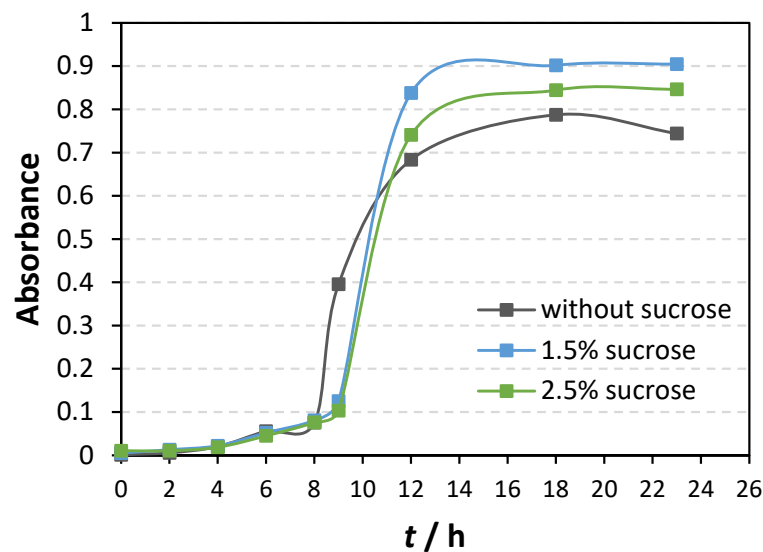


Figure 7. SEM micrographs of the bacteria *S. mutans* after 14 h of incubation time. The micrographs are of composite surfaces with the following sucrose concentrations: (a) 0%, (b) 1.5%, (c) 2.5%, and (d) 5%.

Bacterial Growth Curve of *Streptococcus mutans* Depends upon the Presence or Absence of Sucrose

Since the results demonstrated a significant impact of sucrose on bacterial adhesion, we investigated the growth of *S. mutans* in a solution doped with sucrose (Figure 8). The optical density measurements (Figure 8a) show that adding sucrose reduced the bacterial growth rate in the early hours of bacterial growth. However, after the initial adaptation of the bacteria to the added sucrose, after 8 to 10 h, there was a sudden jump in bacterial growth. After 12 h of incubation, the highest bacterial density was in the suspension with 1.5% sucrose, and the lowest, in that without the addition of sucrose. Additionally, we determined the number of living bacteria during the growth of *S. mutans* (Figure 8b). The results obtained are in agreement with the optical density results for the first 8 h of growth. However, after 8 h of incubation, there was no difference in the number of living bacteria, and the number of bacteria started to decrease.

a)



b)

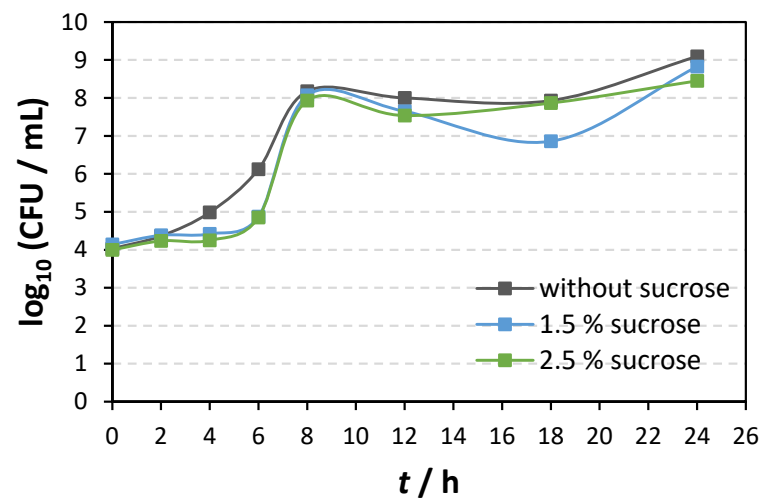


Figure 8. *S. mutans* growth over 24 h with and without sucrose addition as determined (a) with optical density measurements and (b) by counting the number of live bacteria grown on agar plates.

4. Discussion

This study aimed to investigate the impact of varying sucrose concentrations on *S. mutans* adhesion to two common dental material surfaces, a Co-Cr alloy and a resin-based composite.

4.1. Roughness

Surface roughness, measured with a mechanical profilometer, with which five transverse and longitudinal measurements were performed on both types of surfaces of size 1 cm × 1 cm, revealed distinct values for both materials. The resin-based composite surfaces exhibited a larger average roughness, $R_a = 0.32 \pm 0.06 \mu\text{m}$, compared with the Co-Cr alloy, $R_a = 0.21 \pm 0.03 \mu\text{m}$. Higher roughness correlated positively with increased *S. mutans* adhesion, evident in both SEM imaging ($7.08 \pm 0.05\%$) and crystal violet staining ($\text{OD}_{620} = 0.28 \pm 0.06$) on the composite surface. Conversely, Co-Cr demonstrated lower adhesion ($5.94 \pm 0.02\%$ and $\text{OD}_{620} = 0.13 \pm 0.06$). The result is in accordance with the literature, namely, higher surface roughness increases bacterial adhesion. The reason is that greater roughness corresponds to a greater contact surface for bacteria and a greater number of surface defects. In addition, bacteria adhered to rougher surfaces are better protected from shear forces [34–36]. Recently, Kozmos et al. [35] showed that the extent of adhesion of *S. mutans* to composite surfaces was $1.67 \pm 1.03\%$ and that to Co-Cr surfaces was $1.04 \pm 0.23\%$. Carneiro et al. [37] stated that smooth dental implant surfaces extend their lifetime, enhance aesthetic appearance, and reduce dental plaque accumulation on the surface.

4.2. Contact Angle

The hydrophilic nature of both surfaces, indicated by contact angles below 90° , is a crucial factor influencing initial bacterial adhesion. The smaller contact angle observed for the composite ($74.16 \pm 2.95^\circ$) compared with Co-Cr ($76.66 \pm 2.39^\circ$) aligns with studies demonstrating that higher hydrophobicity correlates with increased bacterial adhesion [38]. Loosdrecht et al. [39] have shown that interaction between hydrophobic bacteria and a hydrophobic surface induces higher levels of bacterial adhesion. In a 2021 study, Kozmos et al. compared the adhesion of *S. mutans* to different composite materials. Their study showed that both materials were hydrophilic [35]. Song et al. [40] claim that we can also regulate bacterial adhesion by regulating hydrophobicity. This study shows that an increase in roughness makes hydrophilic surfaces even more hydrophilic.

4.3. Zeta Potential

The zeta potential was measured with the SurPASS electrokinetic analyzer. Most bacteria are negatively charged, so a positively charged surface of the material is more attractive to bacterial adhesion. In contrast, a negative surface is more resistant to bacterial adhesion. A higher zeta potential was measured for the composite ($-25.912 \pm 10.09 \text{ mV}$) and a lower one for Co-Cr ($-52.428 \pm 0.322 \text{ mV}$). Kozmos et al. [35] measured similar negative zeta potentials. It was found that the Co-Cr and composite surfaces were negatively charged, which means that they were more repulsive to the adhesion of *S. mutans*. Excluding the influence of sucrose, we found that the composite, which had a higher zeta potential than Co-Cr, had a higher degree of adhesion in both measurement methods.

4.4. Bacterial Adhesion Extent

In our study, the extent of bacterial adhesion without added sucrose was higher on the composite material than on the Co-Cr alloy (Figure 5). According to a previous study [35], the extent of bacterial adhesion to tooth surfaces was much larger than that to both materials under consideration. In addition to surface roughness and hydrophobicity, surface-specific groups are responsible for relatively high bacterial adhesion. A significantly higher number of adhered bacteria were observed after sucrose addition. Interestingly, the difference in the number of bacteria adhered to the Co-Cr alloy and composite was not visible after adding

sucrose, showing that sucrose significantly influences bacterial adhesion, regardless of the type of material. Here, we have demonstrated that the adhesion extent increases with the increase in sucrose concentration on the Co-Cr alloy and composite surfaces. Moreover, 5% sucrose caused the highest level of bacterial adhesion to the tested surfaces.

Even though the adhesion of bacteria to the surfaces increased with the increase in concentration (Figures 4–7), a different effect was observed in planktonic cells (Figure 8). After prolonged incubation times (12 h and more), the number of dead and alive bacterial cells measured by absorbance was higher at 1.5% of sucrose than at 2.5%. Previous research also showed a decrease in the number of planktonic cells of *S. mutans* [41] and Gram-positive bacteria *Listeria monocytogenes* [42] with an increase in sucrose concentration. The observed decrease in the number of planktonic cells was attributed to an increase in osmotic pressure caused by higher sucrose concentration [41], but the exact mechanism of inhibition was not defined.

The bacterial growth curves (Figure 8) obtained from optical density and CFU count revealed steeper growth curves with sucrose, indicating accelerated cell division. This increased division rate enhances bacterial attachment to surfaces, promoting faster biofilm formation. Although sucrose does not affect the total number of viable cells (Figure 8b), forming more biofilm leads to bacterial competitiveness and more effective bacterial resistance to changes in the biofilm surroundings. Cai et al. showed that sucrose could increase the competitive growth of *S. mutans* in biofilm made of different bacterial strains [41]. Furthermore, bacterial biofilm is more resistant to the effect of antibiotics, disinfectant chemicals, and the body's defense system [43,44]. Understanding the oral biofilm may be an excellent initial point for developing preventive techniques to inhibit biofilm formation and achieve good overall health [45,46].

Sucrose is essential to forming cariogenic biofilms and the subsequent formation of dental caries [16]. Although the choice of material is extremely important for the initial adhesion of bacteria, this research shows that sucrose-rich foods and poor oral hygiene after a meal could help bacteria overcome less favorable surface characteristics and encourage biofilm formation. Clinically, the importance of dietary modifications, especially the reduction in sucrose intake, should be emphasized to mitigate the risk of bacterial adhesion and subsequent biofilm development. Dental practitioners should consider these surface-specific interactions when selecting materials for restorations and prosthetics to minimize the susceptibility to bacterial colonization. Moreover, patient education on the role of dietary choices in oral health may be an integral component of preventive care strategies. The meticulous execution of polishing and finishing procedures in the fabrication of dental composite restorations and metallic prostheses plays a pivotal role in the overall dental restoration process, with profound clinical implications for both the immediate and long-term success of these interventions. The clinician's attention to detail during these procedures is indispensable for mitigating biofilm accumulation, minimizing tissue irritation, upholding marginal integrity, ensuring corrosion resistance (particularly pertinent to metallic prostheses), and fortifying stain resistance. Moreover, the meticulous execution of polishing and finishing procedures is instrumental in achieving optimal esthetic outcomes, fostering patient satisfaction, and enhancing the wear resistance of dental composite restorations and metallic prostheses. Continuous professional development through regular education and training serves as a fundamental mechanism for clinicians to refine their proficiency in these critical facets of dental practice.

5. Conclusions

This study investigated the adhesion of *S. mutans* to commonly used dental materials, namely, a Co-Cr alloy and a resin-based composite, while exploring the influence of varying sucrose concentrations on bacterial adhesion. The results demonstrated that the composite surface is rougher than the Co-Cr alloy surface. Both surfaces are hydrophilic and negatively charged. The extent of bacterial adhesion to Co-Cr surfaces was lower than that to the composite before the addition of sucrose. However, increased sucrose

facilitated faster bacterial division, promoting biofilm formation similarly on both surfaces. A statistically significant impact of sucrose was measured at 2.5%. The highest level of bacterial adhesion was obtained at 5% sucrose in bacterial suspension. This study sheds light on the multifaceted factors influencing *S. mutans* adhesion to dental surfaces and underscores the need for nuanced approaches, both in dental material design and oral hygiene practices, to mitigate the risk of biofilm-associated oral diseases and their potential systemic implications.

Author Contributions: Writing—original draft preparation, K.B.; writing—review and editing F.R., A.Z., N.M.M., J.V., A.U., R.Š., A.P., A.S.Š. and K.B., data analysis: J.V., A.Z., N.M.M. and A.P. All authors have read and agreed to the published version of the manuscript.

Funding: This research received no external funding.

Institutional Review Board Statement: Not applicable.

Informed Consent Statement: Not applicable.

Data Availability Statement: Data are contained within the article.

Acknowledgments: The authors thank ARRS for support through the program “Mechanisms of health maintenance for financial support”. The authors thank ARRS for support through the project “Modulation of fruit polyphenolic profile by sustainable postharvest physical treatments”, J7-2595. The authors thank Zlatarna Celje d.o.o. Slovenia, Kersnikova ulica 19, Celje, for delivering material surfaces. **The authors (Andreja Pondelak and Andrijana Sever Škapin) thank the financial support provided by the Slovenian Research and Innovation Agency (Grants no. P2-0273 and P4-0430).**

Conflicts of Interest: The authors declare no conflicts of interest.

References

- Han, A.; Tsoi, J.K.H.; Rodrigues, F.P.; Leprince, J.G.; Palin, W.M. Bacterial Adhesion Mechanisms on Dental Implant Surfaces and the Influencing Factors. *Int. J. Adhes. Adhes.* **2016**, *69*, 58–71. [[CrossRef](#)]
- Mahler, D.; Sakaguchi, R.L. Restorative Materials—Metals. In *Craig’s Restorative Dental Materials*; Sakaguchi, R.L., Powers, J.M., Eds.; Elsevier Mosby: Philadelphia, PA, USA, 2012; pp. 199–251.
- Lovegrove, J.M. Dental Plaque Revisited: Bacteria Associated with Periodontal Disease. *J. N. Z. Soc. Periodontol.* **2004**, *87*, 7–21.
- Kamel, J.H.; Salman, F.D. Prevalence of Secondary Caries Around Posterior Restoration. *Acta Sci. Med. Sci.* **2022**, *6*, 03–10. [[CrossRef](#)]
- Brouwer, F.; Askar, H.; Paris, S.; Schwendicke, F. Detecting Secondary Caries Lesions. *J. Dent. Res.* **2016**, *95*, 143–151. [[CrossRef](#)]
- Mjör, I.A.; Toffenetti, F. Secondary Caries: A Literature Review with Case Reports. *Quintessence Int.* **2000**, *31*, 165–179. [[PubMed](#)]
- Ionescu, A.C.; Brambilla, E.; Travan, A.; Marsich, E.; Donati, I.; Gobbi, P.; Turco, G.; Di Lenarda, R.; Cadenaro, M.; Paoletti, S.; et al. Silver–Polysaccharide Antimicrobial Nanocomposite Coating for Methacrylic Surfaces Reduces Streptococcus Mutans Biofilm Formation in Vitro. *J. Dent.* **2015**, *43*, 1483–1490. [[CrossRef](#)]
- Veiga, N.; Aires, D.; Douglas, F.; Pereira, M.; Vaz, A.; Rama, L.; Silva, M.; Miranda, V.; Pereira, F.; Vidal, B.; et al. Dental Caries: A Review. *J. Dent. Oral Health* **2016**, *2*, 43–47.
- Islam, B.; Khan, S.N.; Khan, A.U. Dental Caries: From Infection to Prevention. *Med. Sci. Monit.* **2007**, *13*, RA196–RA203.
- Forssten, S.D.; Björklund, M.; Ouweland, A.C. Streptococcus Mutans, Caries and Simulation Models. *Nutrients* **2010**, *2*, 290–298. [[CrossRef](#)] [[PubMed](#)]
- Quirynen, M.; Van Der Mei, H.C.; Bollen, C.M.L.; Schotte, A.; Marechal, M.; Doornbusch, G.I.; Naert, I.; Busscher, H.J.; Van Steenberghe, D. An In Vivo Study of the Influence of the Surface Roughness of Implants on the Microbiology of Supra- and Subgingival Plaque. *J. Dent. Res.* **1993**, *72*, 1304–1309. [[CrossRef](#)]
- Boks, N.P.; Norde, W.; van der Mei, H.C.; Busscher, H.J. Forces Involved in Bacterial Adhesion to Hydrophilic and Hydrophobic Surfaces. *Microbiology* **2008**, *154*, 3122–3133. [[CrossRef](#)] [[PubMed](#)]
- Filipović, U.; Dahmane, R.G.; Ghannouchi, S.; Zore, A.; Bohinc, K. Bacterial Adhesion on Orthopedic Implants. *Adv. Colloid Interface Sci.* **2020**, *283*, 102228. [[CrossRef](#)] [[PubMed](#)]
- Abranches, J.; Zeng, L.; Kajfasz, J.K.; Palmer, S.R.; Chakraborty, B.; Wen, Z.T.; Richards, V.P.; Brady, L.J.; Lemos, J.A. Biology of Oral Streptococci. *Microbiol. Spectr.* **2018**, *6*, 42–60. [[CrossRef](#)] [[PubMed](#)]
- Lemos, J.A.; Palmer, S.R.; Zeng, L.; Wen, Z.T.; Kajfasz, J.K.; Freires, I.A.; Abranches, J.; Brady, L.J. The Biology of Streptococcus Mutans. *Microbiol. Spectr.* **2019**, *7*, 56–69. [[CrossRef](#)] [[PubMed](#)]
- Negrini, T.d.C.; Ren, Z.; Miao, Y.; Kim, D.; Simon-Soro, Á.; Liu, Y.; Koo, H.; Arthur, R.A. Dietary Sugars Modulate Bacterial-Fungal Interactions in Saliva and Inter-Kingdom Biofilm Formation on Apatitic Surface. *Front. Cell. Infect. Microbiol.* **2022**, *12*, 993640. [[CrossRef](#)] [[PubMed](#)]

17. Van Amerongen, J.P.; Watson, T.F.; Opdam, N.J.M.; Roeters, F.J.M. Restoring the Tooth: «The Seal Is the Deal». In *Dental Caries: The Disease and Its Clinical Management*; Fejerskov, O., Kidd, E.A.M., Eds.; Blackwell: Oxford, UK, 2008; pp. 387–395.
18. Cai, J.-N.; Jung, J.-E.; Dang, M.-H.; Kim, M.-A.; Yi, H.-K.; Jeon, J.-G. Functional Relationship between Sucrose and a Cariogenic Biofilm Formation. *PLoS ONE* **2016**, *11*, e0157184. [[CrossRef](#)]
19. Grosogeat, B.; Vaicelyte, A.; Gauthier, R.; Janssen, C.; Le Borgne, M. Toxicological Risks of the Cobalt–Chromium Alloys in Dentistry: A Systematic Review. *Materials* **2022**, *15*, 5801. [[CrossRef](#)]
20. Al Jabbari, Y.S. Physico-Mechanical Properties and Prosthodontic Applications of Co-Cr Dental Alloys: A Review of the Literature. *J. Adv. Prosthodont.* **2014**, *6*, 138–145. [[CrossRef](#)]
21. Yeung, A.L.P.; Lo, E.C.M.; Chow, T.W.; Clark, R.K.F. Oral Health Status of Patients 5–6 Years after Placement of Cobalt-Chromium Removable Partial Dentures. *J. Oral Rehabil.* **2000**, *27*, 183–189. [[CrossRef](#)]
22. Sulistiani, D.A.; Widjijono, W.; Dharmastiti, R. Bacterial Adhesion of Streptococcus Mutans to Cobalt Chromium Recast Alloys. *Maj. Kedokt. Gigi Indones.* **2022**, *7*, 84. [[CrossRef](#)]
23. Vaicelyte, A.; Janssen, C.; Le Borgne, M.; Grosogeat, B. Cobalt–Chromium Dental Alloys: Metal Exposures, Toxicological Risks, CMR Classification, and EU Regulatory Framework. *Crystals* **2020**, *10*, 1151. [[CrossRef](#)]
24. Yildirim Üçüncü, M.; Kazım ÜÇÜNCÜ, M. Comparison of the Mechanical Properties of Various Microhybrid Dental Composites. *Euroasian Dent. Res.* **2023**, *1*, 58–64.
25. Motevasselian, F.; Zibafar, E.; Yassini, E.; Mirzaei, M.; Pourmirhoseni, N. Adherence of Streptococcus Mutans to Microhybrid and Nanohybrid Resin Composites and Dental Amalgam: An In Vitro Study. *J. Dent.* **2017**, *14*, 337–343.
26. Tuncer, S.; Demirci, M.; Öztaş, E.; Tekçe, N.; Uysal, Ö. Microhybrid versus Nanofill Composite in Combination with a Three Step Etch and Rinse Adhesive in Occlusal Cavities: Five Year Results. *Restor. Dent. Endod.* **2017**, *42*, 253. [[CrossRef](#)] [[PubMed](#)]
27. Silva, R.A.B.; Nelson-Filho, P.; De-Oliveira, K.M.H.; Romualdo, P.C.; Gatón-Hernandez, P.; Aires, C.P.; Silva, L.A.B. Adhesion and Initial Colonization of Streptococcus Mutans Is Influenced by Time and Composition of Different Composites. *Int. J. Odontostomatol.* **2018**, *12*, 395–400. [[CrossRef](#)]
28. Heintze, S.D.; Loguercio, A.D.; Hanzen, T.A.; Reis, A.; Rousson, V. Clinical Efficacy of Resin-Based Direct Posterior Restorations and Glass-Ionomer Restorations—An Updated Meta-Analysis of Clinical Outcome Parameters. *Dent. Mater.* **2022**, *38*, e109–e135. [[CrossRef](#)]
29. Maran, B.M.; de Geus, J.L.; Gutiérrez, M.F.; Heintze, S.; Tardem, C.; Barcelheiro, M.O.; Reis, A.; Loguercio, A.D. Nanofilled/Nanohybrid and Hybrid Resin-Based Composite in Patients with Direct Restorations in Posterior Teeth: A Systematic Review and Meta-Analysis. *J. Dent.* **2020**, *99*, 103407. [[CrossRef](#)]
30. de Andrade, A.; Duarte, R.; Medeiros e Silva, F.D.; Batista, A.; Lima, K.; Monteiro, G.; Montes, M. Resin Composite Class I Restorations: A 54-Month Randomized Clinical Trial. *Oper. Dent.* **2014**, *39*, 588–594. [[CrossRef](#)]
31. Sirin Karaarslan, E.; Aytac Bal, F.; Buldur, M.; Altan, H. Twenty-Four-Month Clinical Comparison of Two Bulk-Fill and a Microhybrid Composite Restorations in Class II Cavities. *Eur. J. Prosthodont. Restor. Dent.* **2021**, *29*, 231–240. [[CrossRef](#)] [[PubMed](#)]
32. Huang, H. Ion Release from NiTi Orthodontic Wires in Artificial Saliva with Various Acidities. *Biomaterials* **2003**, *24*, 3585–3592. [[CrossRef](#)] [[PubMed](#)]
33. Nozaki, K.; Koizumi, H.; Horiuchi, N.; Nakamura, M.; Okura, T.; Yamashita, K.; Nagai, A. Suppression Effects of Dental Glass-Ceramics with Polarization-Induced Highly Dense Surface Charges against Bacterial Adhesion. *Dent. Mater. J.* **2015**, *34*, 671–678. [[CrossRef](#)]
34. Gharechahi, M.; Moosavi, H.; Forghani, M. Effect of Surface Roughness and Materials Composition. *J. Biomater. Nanobiotechnol.* **2012**, *3*, 541–546. [[CrossRef](#)]
35. Kozmos, M.; Virant, P.; Rojko, F.; Abram, A.; Rudolf, R.; Raspor, P.; Zore, A.; Bohinc, K. Bacterial Adhesion of Streptococcus Mutans to Dental Material Surfaces. *Molecules* **2021**, *26*, 1152. [[CrossRef](#)] [[PubMed](#)]
36. Teughels, W.; Van Assche, N.; Sliepen, I.; Quirynen, M. Effect of Material Characteristics and/or Surface Topography on Biofilm Development. *Clin. Oral Implants Res.* **2006**, *17*, 68–81. [[CrossRef](#)] [[PubMed](#)]
37. Carneiro, P.; Ramos, T.; de Azevedo, C.; de Lima, E.; de Souza, S.; Turbino, M.; Cesar, P.; Matos, A. Influence of Finishing and Polishing Techniques and Abrasion on Transmittance and Roughness of Composite Resins. *Oper. Dent.* **2016**, *41*, 634–641. [[CrossRef](#)] [[PubMed](#)]
38. Azam, M.; Khan, A.; Muzzafar, D.; Faryal, R.; Siddiqi, S.; Ahmad, R.; Chauhdry, A.; Rehman, I. Structural, Surface, in Vitro Bacterial Adhesion and Biofilm Formation Analysis of Three Dental Restorative Composites. *Materials* **2015**, *8*, 3221–3237. [[CrossRef](#)]
39. van Loosdrecht, M.C.; Lyklema, J.; Norde, W.; Schraa, G.; Zehnder, A.J. The Role of Bacterial Cell Wall Hydrophobicity in Adhesion. *Appl. Environ. Microbiol.* **1987**, *53*, 1893–1897. [[CrossRef](#)] [[PubMed](#)]
40. Song, F.; Koo, H.; Ren, D. Effects of Material Properties on Bacterial Adhesion and Biofilm Formation. *J. Dent. Res.* **2015**, *94*, 1027–1034. [[CrossRef](#)]
41. Cai, J.-N.; Choi, H.-M.; Jeon, J.-G. Relationship between Sucrose Concentration and Bacteria Proportion in a Multispecies Biofilm. *J. Oral Microbiol.* **2021**, *13*, 1910443. [[CrossRef](#)] [[PubMed](#)]
42. Meldrum, R.J.; Brocklehurst, T.F.; Wilson, D.R.; Wilson, P.D.G. The Effects of Cell Immobilization, PH and Sucrose on the Growth of *Listeria Monocytogenes* Scott A at 10 °C. *Food Microbiol.* **2003**, *20*, 97–103. [[CrossRef](#)]

43. Høiby, N.; Bjarnsholt, T.; Givskov, M.; Molin, S.; Ciofu, O. Antibiotic Resistance of Bacterial Biofilms. *Int. J. Antimicrob Agents* **2010**, *35*, 322–332. [[CrossRef](#)] [[PubMed](#)]
44. Stewart, P.S.; William Costerton, J. Antibiotic Resistance of Bacteria in Biofilms. *Lancet* **2001**, *358*, 135–138. [[CrossRef](#)]
45. Contardo, M.S.; Díaz, N.; Lobos, O.; Padilla, C.; Giacaman, R.A. Oral Colonization by Streptococcus Mutans and Its Association with the Severity of Periodontal Disease in Adults. *Rev. Clin. Periodoncia Implantol. Rehabil. Oral* **2011**, *4*, 9–12. [[CrossRef](#)]
46. Dani, S.; Prabhu, A.; Chaitra, K.; Desai, N.; Patil, S.; Rajeev, R. Assessment of Streptococcus Mutans in Healthy versus Gingivitis and Chronic Periodontitis: A Clinico-Microbiological Study. *Contemp. Clin. Dent.* **2016**, *7*, 529. [[CrossRef](#)] [[PubMed](#)]

Disclaimer/Publisher’s Note: The statements, opinions and data contained in all publications are solely those of the individual author(s) and contributor(s) and not of MDPI and/or the editor(s). MDPI and/or the editor(s) disclaim responsibility for any injury to people or property resulting from any ideas, methods, instructions or products referred to in the content.